Atmos. Chem. Phys. Discuss., 6, 6369–6399, 2006
www.atmos-chem-phys-discuss.net/6/6369/2006/

Atmospheric Chemistry and Physics Discussions

Investigating the composition of organic aerosol resulting from cyclohexene ozonolysis: low molecular weight and heterogeneous reaction products

J. F. Hamilton[1], A. C. Lewis[1], J. Reynolds[1], L. J. Carpenter[1], and A. Lubben[2]

[1]Department of Chemistry, University of York, Heslington, York, YO10 5DD, UK
[2]Bruker Daltonics, Banner Lane, Coventry, CV4 9GH, UK

Received: 26 April 2006 – Accepted: 16 May 2006 – Published: 12 July 2006

Correspondence to: J. F. Hamilton (jfh2@york.ac.uk)

Abstract

The composition of organic aerosol formed from the gas phase ozonolysis of cyclohexene has been investigated in a smog chamber experiment. Comprehensive gas chromatography with time of flight mass spectrometric detection was used to determine that dicarboxylic acids and corresponding cyclic anhydrides dominated the small gas phase reaction products found in aerosol sampled during the first hour after initial aerosol formation. Structural analysis of larger more polar molecules was performed using liquid chromatography with ion trap tandem mass spectrometry. This indicated that the majority of identified organic mass was in dimer form, built up from combinations of the most abundant small acid molecules, with frequent indication of the inclusion of adipic acid. Trimers and tetramers potentially formed via similar acid combinations were also observed in lower abundances. Tandem mass spectral data indicated dimers with either acid anhydride or ester functionalities as the linkage between monomers. High-resolution mass spectrometry identified the molecular formulae of the most abundant dimer species to be $C_{10}H_{16}O_6$, $C_{11}H_{18}O_6$, $C_{10}H_{14}O_8$ and $C_{11}H_{16}O_8$ and could be used in some cases to reduce uncertainty in exact chemical structure determination by tandem MS.

1 Introduction

It has recently been established that significant amounts of particulate matter are organic in nature deriving from both primary and secondary sources, where organic material can contribute 20–50% of the total fine (sub-micron) aerosol mass in continental mid-latitudes (Putaud et al., 2004; Saxena et al., 1996) and up to 90% in tropical highly forested areas (Andreae et al., 1997; Artaxo et al., 1988; Talbot et al., 1988). Volatile organic compounds (VOCs) are emitted to the atmosphere from both biogenic and anthropogenic sources, which within the boundary layer of the troposphere have the ability to react rapidly with NO_x in the presence of OH radicals (formed from sunlight) to

form ozone and other photochemical by-products. Secondary organic aerosol (SOA) can form in the atmosphere following the photo-oxidation of these gas phase organic species which often result in the formation of lower vapour pressure products. In order to understand and predict the growth and ageing of SOA, and its subsequent radiative and hygroscopicity characteristics, it is necessary to understand both the chemical nature of SOA precursors, and the end products and mechanisms by which SOA is formed.

Partitioning of organic compounds to the aerosol phase and subsequent reactions both on the aerosol surface and within the bulk particle are currently poorly understood. In previous studies of speciation of organics in SOA, the observation of compounds whose vapour pressure should prohibit their incorporation into the aerosol could not be explained (Forstner et al., 1997; Jang et al., 2001). More recently however, high molecular weight and hence low volatility, organic species have been found in aerosol formed during smog chamber studies from a range of precursors (Kalberer et al., 2004). It has been suggested that heterogeneous reactions, both on the surface and within the bulk, may aid the incorporation of volatile compounds, producing stable macromolecules or polymers within the aerosol. The nature of this low volatility fraction and its formation reactions are still highly uncertain however.

High molecular weight reaction products have been identified in aged SOA from a wide range of compounds, including 1,3,5-trimethyl-benzene, cyclo-alkenes, α-pinene and glyoxal (Bahreini et al., 2005; Gao et al., 2004a; Hastings et al., 2005; Kalberer et al., 2004, 2005). Initial evidence provided a size distribution using Laser Desorption Ionisation Mass Spectrometry (LDI-MS) (Kalberer et al., 2004), but this approach was unable to provide detailed structural information. Tolocka et al. (2004) applied liquid chromatography combined with matrix laser desorption ionisation (MALDI), electrospray ionisation (ESI) and chemical ionisation (CI) mass spectrometry. CI was found to cause decomposition of the parent oligomer, but MALDI and ESI provided similar oligomer distributions. Tandem mass spectrometry using a quadrupole time of flight (Q-TOF) allowed structural identification of individual compounds including dimers, trimers

and tetramers of known gas phase reaction products from the ozonolysis of α-pinene. Currently however only a very limited number of VOCs have been tested as precursors and little information on exact oligomers structures and hence formation mechanisms are available.

Cyclohexene is emitted to the atmosphere from both anthropogenic and natural sources. Reaction of cyclohexene with ozone can occur in dark conditions and is a known night time source of OH radicals. Although of relatively low individual abundance in the atmosphere it has been studied in the laboratory extensively, since it acts as a simple surrogate for the behaviour of more complex terpenoid species. Limited information is available on the composition of SOA produced from this reaction but a number of recent studies have shown the occurrence of oligomers in aged aerosol (4–6 h after start of reaction) (Bahreini et al., 2005; Gao et al., 2004a, b).

This paper describes a detailed analysis of chemicals found within SOA formed during a cyclohexene ozonolysis reaction in the European Photo-reactor (EUPHORE) chamber. Three complimentary state of the art analytical techniques were used to identify the composition of cyclohexene SOA including both early generation gas phase reaction products (i.e. the monomer building blocks) and higher molecular weight products, formed from heterogeneous reactions either on the surface or within the bulk of the aerosol. Thermal desorption coupled to comprehensive gas chromatography with time-of-flight mass spectrometry (GCXGC-TOF/MS) has previously been used to identify small molecules in toluene photo-oxidation SOA and has been used in this study (Hamilton et al., 2005). A technique to identify oligomers in SOA using reverse phase liquid chromatography with electrospray ionisation and ion-trap mass spectrometry (LC-ESI-MS/MS) was developed and the results are presented. Empirical formulae were subsequently determined for the major components identified in LC-ESI-MS/MS using liquid chromatography coupled to high mass accuracy Time-of-Flight MS (LC-ESI-TOF)

2 Experimental

Experiments were carried out at the European Photo-Reactor (EUPHORE) in Valencia, Spain, which consists of two FEP-Teflon hemispheres, each with a volume of approximately 200 m^3. The floor is water-cooled to minimise solar heating and an air purification and drying system provides NO_y-NMHC-free and dry air while two fans ensure homogenous mixing of the chamber air. The initial concentrations of cyclohexene and ozone were 120 ppb and 420 ppb, respectively. Excess *i*-propanol (8 ml) was used as an OH scavenger. Samples were collected on 47 mm diameter quartz-fibre filters using a high volume sample pump. Filters were pre-fired at 500 ^oC for 12 hours prior to sample collection, and were stored in a sealed vial below 4 ^oC until analysis. Samples were collected at approximately 74.4 L min^{-1} for 60 min, with a total sample volume of 4.21 m^3 and the total mass of aerosol collected onto the filter was 794 μg.

An area of approximately 3 mm×9 mm was removed from the filter and cut into three equal sized pieces for analysis by GCXGC. The small section of filter paper was introduced into a cooled glass GC injection liner (50°C), purged with helium and then heated at 20°C min^{-1} in a flow of helium to a maximum of 300°C, where it was held for 10 min. The organics released in this heating regime were collected in a silica capillary liquid nitrogen cold trap inside the GC oven. Following desorption from the aerosol matrix, the silica capillary trap was removed from the liquid nitrogen and rapidly heated to the oven temperature. Further details can be found elsewhere (Hamilton et al., 2004). GCXGC-TOF/MS was carried out using a cryo-jet Pegasus 4D (Leco, St. Joseph, MI, USA) incorporating an Agilent 6890N Gas Chromatograph and a Pegasus III reflectron time-of-flight mass spectrometer. A liquid nitrogen cooled gas jet midpoint modulator, at approximately –160°C, was used to enable comprehensive two-dimensional separations. A secondary oven housed within the GC oven allowed independent column temperature controls. The columns set used in experiments provides a primary volatility based separation followed by a secondary polarity based separation. The first dimension was a 5% phenyl-95% methyl-polysiloxane 30 m×320 μm×1.0 μm HP-5 (J&W

Scientific, Wilmington, DE, USA). The second column was a 14% cyanopropylphenyl-polysiloxane 2 m×100 μm×0.1 μm BP10 (SGE, Melbourne, Australia). The GC was held at 70°C for two minutes and then raised at 2.5°C min^{-1} to 250°C and held at this temperature for a further sixteen minutes. The carrier gas was helium (99.9999%, BOC Gases, Guilford, UK) supplied at 1.5 ml min^{-1}. The modulator and secondary oven were operated at +30°C and +15 ^oC above GC oven temperature, respectively.

The remainder of the filter was placed into 5 ml of HPLC grade methanol (Fisher Scientific, Hampton, NH, USA), the sample vial wrapped in foil to avoid photolysis and left for two hours. This was sonicated for one hour and the methanol extraction filtered using a 0.45 mm PVDF syringe filter (Whatman). The extract was blown to dryness under a gentle stream of nitrogen and the residue re-dissolved in 1 ml of 0.1% formic acid in HPLC-MS grade water (Riedel-de Haën, Germany) 50% methanol solution. LC-MS/MS analysis was performed using a HCT Plus ion trap mass spectrometer (Bruker Daltonics GmbH, Bremen, Germany) equipped with an Eclipse ODS-C_{18} column with 5 μm particle size (Agilent, 4.6 mm×150 mm). Samples (40 μl) were injected via an autosampler (Agilent 1100 series) and a gradient elution was performed using 0.1% formic acid in HPLC-MS grade water (75% to 40% over fifteen minutes, hold for ten minutes, return to starting conditions) and pure methanol at 0.6 ml min^{-1}. Electrospray ionisation was carried out at 300°C, with a nebuliser pressure of 50 psi and nitrogen dry gas flow rate of 12 L min^{-1}. The mass spectrometer was used in alternating positive and negative ion mode, scanning from 50 to 1000 Daltons (Da).

High resolution TOF measurements were performed using an electrospray micrOTOF (Bruker Daltonics GmbH, Germany). Chromatographic conditions were identical to those used previously. 10 μl aliquots of the samples were injected via an autosampler (Agilent 1100 series). Negative ion electrospray ionisation was carried out at a source temperature of 200°C, nebuliser pressure of 14 psi and a nitrogen dry gas flow rate of 7 l min^{-1}. The scan range used was 50 to 800 Da. The data was externally calibrated using an average spectrum of sodium formate clusters automatically injected at the start of the chromatographic run.

3 Results

3.1 GCXGC analysis

Initial analysis of the cyclohexene SOA was carried out using thermal desorption coupled to GCXGC-TOF/MS and an example chromatogram is shown in Fig. 1. The chromatogram is presented as a contour plot with the retention times on columns 1 and 2 on the X- and Y-axis and the response as a coloured contour. Each spot on the chromatograms represents an individual compound with a full mass spectrum. Increasing retention times on columns one and two indicate increasing volatility and polarity, respectively. A total of 45 analytes were identified and structures are given in Table 1.

The chromatogram is dominated by di-carboxylic acids (glutaric C_5 and adipic C_6) and their corresponding cyclic anhydrides. The majority of the identified mass is accounted for by a small number of compounds, unlike previous studies of toluene SOA where no one compound or functionality dominated (Hamilton et al., 2005). In addition, a number of ring-retained compounds were identified, including cyclohexanone, cyclohexanol, 1,2-cyclohexandiol, 1,2-cyclohexandione and 2-hydroxy-cyclohexanone, which can be mechanistically linked directly to the starting reactant. Large numbers of cyclic products, formed via a ring cleavage process, were also found including both 5 and 6 membered rings such as cyclopentanones, cyclopentenones, lactones, pyranones and bicyclic species. Dihydro-2(3H)-furanone and tetrahydro-2H-pyran-2-one are most likely the result of dehydration and internal cyclisation of the corresponding terminal hydroxy-acid (4-hydroxy-butanoic acid and 5-hydroxy-pentanoic acid) which is known to occur rapidly on formation (Kimura et al., 2003).

Many previous studies of SOA composition use derivatization to convert polar groups to less polar functionalities to make them more suitable for GC analysis. Popular derivatization agents used include PFBHA (O-(2,3,4,5,6-pentafluorobenzyl)-hydroxamine) and BSTFA (N,O-bis(trimethylsilyl)-trifluoroacetamide), which convert carbonyl groups and carboxyl/hydroxyl groups, respectively. The derivatized analytes are well suited to GC and produce good peak characteristics although cyclic compounds, such as those

identified in this study, do not react with these derivatization compounds and would potentially not be resolved. In this work the use of thermal desorption to release semi-polar compounds from the aerosol removes the use of polar solvents which can cause solvent effects (such as peak tailing, broadening or splitting) and hence the loss or reaction of compounds during GC analysis (Fowlis, 1995). Thermal desorption and GC in general has a limited polarity range, obvious in the tailing peak shape of glutaric and adipic acid in Fig. 1. More volatile di-acids, such as oxalic and malonic acid cannot be identified using this technique as they are lost to surfaces within the liner and degrade on column.

A number of unidentified peaks were found with this technique and interpretation of their mass spectra proved inconclusive. However, fragmentation patterns with losses of 14 (CH_2), 16 (O) and 28 (CO) mass units suggest an oxidised hydrocarbon backbone. Compounds with fragments as large as 166 Da were seen, and cannot be accounted for without "mass adding" heterogeneous reactions.

3.2 LC-ESI MS/MS analysis

The methanol extracts of cyclohexene SOA were analysed using LC-MS/MS in both the negative and positive ionisation modes and the base peak chromatograms are shown in Fig. 2. The base peak chromatogram is a representation of the most intense single ion at each scan point and this ion mass is shown for each peak. A blank filter was also extracted but the chromatogram showed no significant peaks above the noise. Positive ionisation mode had the highest sensitivity but the majority of ions had formed adducts with Na^+ and K^+, which provided poor fragmentation patterns and was not used further in this study.

Analytes with molecular masses below 200 Da dominate the early part of the chromatogram. Structural analysis of fragmentation patterns and comparison with standard solutions resulted in the detection of 7 low molecular weight acids. Peak identifications are shown in Table 2 and correspond to the following products: glutaric acid, adipic acid, 6-oxohexanoic acid, 3,6-dihydroxy-5-oxohexanoic acid, di-oxohexanoic

acid, hydroxy-glutaric acid and hydroxy-adipic acid. The position of the hydroxyl or carbonyl group on the final three analytes cannot be determined using this technique. The most abundant molecules found during the GCXGC analysis, i.e. the di-acids and their derivatives, also account for the majority of small molecules identified in the LC analysis, highlighting the complimentary nature of the two techniques.

These acids have previously been identified as some of the major components of SOA formed during cyclohexene ozonolysis and can be mechanistically linked to the parent hydrocarbon, via a number of reaction pathways. A total of 16 di-carboxylic acids, hydroxy-acids, oxo-acids, di-aldehydes and pentanal were quantified in Kalberer et al. (2000) and were found to account for almost all of the aerosol volume, based on an aerosol density of 1.4 g cm^{-3}. Gao et al. (2004a) identified a total of 20 low molecular weight species in cyclohexene-O_3 SOA, which were calculated to account for 42% of the total SOA mass. A further 3% was attributed to oligomeric structures. This discrepancy was attributed partly to the use of different OH scavengers (CO versus cyclohexane) producing different HO_2 to RO_2 ratios in the reaction system. This study uses *i*-propanol as the OH scavenger, so is different from either study. Other factors that may produce artifacts include the use of denuders, different filters and sampling preparation techniques.

Although no direct quantification was carried out in this study (since for many species no standard or authentic compound exists), it is clear from Fig. 2 that these early generation ozonolysis products account for perhaps less than half of the overall aerosol composition. The intensity of the base peak chromatograms suggests that the majority of compounds identified have a molecular mass greater than 200 Da and are likely the result of combination reactions either heterogeneously with the aerosol or in the gas phase. The dotted line on the chromatograms indicates the shift from small monomer type compounds to dimers, formed using the monomer building blocks. Using a tandem MS approach with an ion-trap, the two most abundant ions at each survey scan at any point on the chromatogram are isolated and undergo one stage of collision induced fragmentation (MS^2). Using the product ion mass spectra (i.e. MS^2), a detailed struc-

tural analysis of each peak was carried out and confirmed the most abundant peaks as dimers.

The four most abundant dimers found correspond to precursor ion masses of 231, 245, 261 and 275 m/z and the MS and product ion mass spectra are shown in the top half of Figs. 3–6. Due to the limited number of fragment ions produced for these species an exact structural identification could not be obtained, only a reduction in possible chemical structure possibilities. Sufficient data was available to determine the possible molecular formulas for each peak, shown in Table 3. Each molecular formula is accompanied by one of the most likely dimer structures, assuming they are composed of the most abundant low molecular weight compounds identified in the SOA using GCXGC and LC-MS. The monomer pair that would form the example structures are also shown in Table 3. In some cases, such as the $C_7H_2O_{10}$ molecular formula for M=246 Da, the chemical structure given is the only possible isomer.

The largest peak in the chromatogram corresponds to a $[M\text{-}H]^-$ of 245 Da and the mass spectrum and product ion mass spectrum are shown in the top half of Fig. 3. The 245 ion dissociates to the fragment ions of 145, 127, 117, 101, 83 Da and two structures, with different molecular formulas, that fit the required fragments are shown in the lower half of Fig. 3. In the case of all the possible molecular formulae, the linkage between the monomer units is either ester or anhydride functionality. Although the end groups may have differing combinations of C, H and O, to match the mass spectrum, the linkage can only be via one of these two functional groups. In practice the spectra could well be composed of both functional types as a mixture.

The mass resolution of the ion-trap mass spectrometer is insufficient to differentiate between the five proposed molecular formulae for $[M\text{-}H]^-$=245 Da. However, due to the different atomic combinations, they have slightly different accurate mass values e.g. $C_{11}H_{18}O_6$=246.261726 and $C_7H_2O_{10}$=246.087894 Da. The cyclohexene extract was analysed on a micrOTOF, a time-of-flight mass spectrometer with a resolution of 10 000. This allows the measurement of accurate mass to 1 mDa, and to differentiate between two ions of very similar mass. As the isobaric compounds were separated in

time by chromatography, the resolution aspect was less important than the accurate mass. The spectra contained information not only on the accurate mass, but also isotope ratios. The combinations of these two pieces of information were used to narrow down a theoretical list of potential formula to give a confident compound identification.

Using accurate mass measurements, the molecular formula of the most abundant compound with M=246 Da was confirmed as $C_{11}H_{18}O_6$. With this information and the MS^2 fragmentation data in both the negative and positive ionisation modes, the only possible linkage of the two reactants is an ester, with the most likely structure being a dimer of adipic acid and 5-hydroxy-pentanoic acid. The extracted ion chromatogram obtained on the micrOTOF for $[M\text{-}H]^-$=245 Da is shown in Fig. 7. Although the $C_{11}H_{18}O_6$ peak is the largest in the chromatogram, more oxidised compounds are also present, and their possible structures are given in Table 3. MS^2spectra are not available for these compounds due co-elution with more abundant ions.

Accurate mass measurement and the product ion mass spectrum for [M-H]=231 Da, indicate that this compound is an analogue of the previous dimer, with one less CH_2 group i.e. $C_{10}H_{16}O_6$. Combining accurate mass and tandem MS data again gives the most likely structure as the ester of glutaric acid and 5-hydroxy-pentanoic acid, shown in Fig. 4.

The next most abundant peaks correspond to 261 and 275 Da ions. Accurate mass measurements indicate these compounds are more oxidised both containing 8 oxygen atoms ($C_{10}H_{14}O_8$ and $C_{11}H_{16}O_8$, respectively). The linkage between monomers units can be either an ester or an acid anhydride depending on the position of the carbonyl groups and example structures are shown in Figs. 5 and 6. The combination of MS techniques in this case is unable to determine exactly the linkage only refine to two possibilities or a combination thereof. It is clear that the composition of heterogeneous reaction products is reasonably complex, with single ion masses being most likely made up of a mixture of different molecular formulas. The power of LC is certainly required to isolate individual compounds with the same nominal mass but varying degrees of oxidation, which are not possible using techniques based on ionisation alone.

Although the main peaks identified from tandem MS correspond generally to the least oxidised structures in Table 3, high resolution mass spectrometry indicates that the majority of molecular formulas proposed in Table 3 are present in this SOA.

The smaller peaks at the end of the separation are difficult to see above the noise, with many low concentration species eluting together to give an elevated baseline. Plotting single ion chromatograms allows individual peaks to be extracted from this baseline. The region of the chromatogram between 15 and 24 min has been expanded and individual ion chromatograms for 4 masses are shown in Fig. 8. These later peaks correspond to molecules with a molecular mass greater than 300 Da. The product ion mass spectra for the four peaks are shown in the lower region of Fig. 8. The product ion mass spectra have a common set of product ions – 145, 217 and 245 Da – indicating that they have related structures. Indeed the 145 fragment corresponds to an ionised [M-H] adipic acid group and is seen in many of the dimers also. Structural analysis of the product ion mass spectra is inconclusive but suggests that these peaks are mixtures of trimers and tetramers, which cannot be individually separated by the LC system used here.

In order to obtain a profile of the total molecular mass distribution of SOA components, the average mass spectra across the entire chromatogram can be combined. This approach provides a "view" of chemical composition similar to that obtained using techniques such as MALDI. A comparison of the mass distribution profiles (negative ion mode) from the extracted blank filter and the cyclohexene SOA are shown in Fig. 9. This average mass spectra is very similar to that obtained by directly infusing the sample into the ESI-ion trap without any LC separation. The blank filter provides a background mass spectrum, where there is no obvious structure, the maximum intensity is 600 counts and most masses are below 400 counts. The cyclohexene SOA mass spectrum shows the expected major larger ion peaks 14 (CH_2) and 16 (O) Da apart. The high intensity 131, 145 and 161 Da ions correspond to glutaric acid, adipic acid and hydroxy-adipic acid identified earlier. The monomer and dimers dominate the mass spectrum (in the same way they dominate when viewed as individual chromato-

graphic peaks) but it is clear that a significant amount of aerosol mass resides in an oligomeric form, with ion fragments above the background up to at least 600 Da. These oligomeric compounds are found in low concentrations and do not undergo MS^2 fragmentation, due to overlapping with more abundant analytes during the LC separation and insufficient sensitivity of the ion-trap during syringe infusion. The SOA resolved in this paper was produced during the first hour after initial aerosol was detected and indicates that heterogeneous reactions do begin to occur early in the formation and aging process. Although the monomer and dimers dominate the SOA composition, within an hour molecules up to 600 Da have already formed.

The total chromatogram mass spectra shown in Fig. 9 can also be plotted for the product ion mass spectra to give an indication of the most common fragments/monomers. The $\sum MS^2$ was plotted for the monomer-dimer (Rt 2.0-Rt 16.0) and trimer-tetramer (Rt 16-Rt 32.8) regions of the chromatogram and are shown in Fig. 10. The monomer-dimer product ion mass spectrum is dominated by fragment 145 Da (adipic acid) and other low molecular weight species. The trimers-tetramers spectrum shows both monomer and dimer groups, and is again dominated by 145 Da (and its fragmentation products – loss of $-OH_2$=127 Da, loss of –CO=101 Da and loss $-OH_2$+CO=83 Da). It is clear that although the SOA composition formed from this precursor ion is time consuming to resolve, only a limited number of key chemical fragments are needed to describe much of the composition. This demonstrates that only a small subset of possible early stage small molecule SOA products found in the GCXGC and LC analysis take part in the heterogeneous reactions in the early stages of aerosol processing, – in this case of cyclohexene it is adipic acid that is commonly incorporated to larger molecules. This would suggest that in the future it may prove feasible to construct a detailed precursor specific chemical SOA formation scheme in the manner used in master chemical mechanisms for the gas phase.

4 Conclusions

The composition of the secondary organic aerosol formed during the ozonolysis of cyclohexene has been investigated and it was determined that the majority of the organic mass was composed of di-carboxylic acids, cyclic anhydrides and dimer molecules, formed through reactions of the most abundant small acids. Tandem mass spectrometry indicated the predominate linkage between monomer units as either esters or acid anhydrides. Trimers and tetramers were identified but could not be structurally assigned. High resolution mass spectrometry allowed the exact molecular formulas of the most abundant dimers to be determined, structures which can only be accounted for by mass adding heterogeneous reactions. Although the aerosol analysed was collected relatively early in the aging process, molecules up to 600 Da were found. Fragmentation of larger molecules produced a limited number of product ions, indicating that only a subset of gas phase reaction products undergo heterogeneous reactions.

Acknowledgements. Thanks go to K. Wirtz and the team at the Fundación Centro de Estudios Ambientales del Mediterráneo (CEAM) in Valencia, Spain. Thanks to Bruker Daltonics for high-resolution mass spectrometric analysis. This research was funded by the NERC grant (NE/B50582X/1).

References

Andreae, M. O. and Crutzen, P. J.: Atmospheric aerosols: Biogeochemical sources and role in atmospheric chemistry, Science, 276, 1052–1058, 1997.

Artaxo, P., Storms, H., Bruynseels, F., Vangrieken, R., and Maenhaut, W.: Composition and Sources of Aerosols from the Amazon Basin, J. Geophys. Res., 93, 1605–1615, 1988.

Bahreini, R., Keywood, M. D., Ng, N. L., Varutbangkul, V., Gao, S., Flagan, R. C., Seinfeld, J. H., Worsnop, D. R., and Jimenez, J. L.: Measurements of secondary organic aerosol from oxidation of cycloalkenes, terpenes, and m-xylene using an Aerodyne aerosol mass spectrometer, Env. Sci. Techol., 39, 5674–5688, 2005.

Forstner, H. J. L., Flagan, R. C., and Seinfeld, J. H.: Secondary organic aerosol from the photooxidation of aromatic hydrocarbons: Molecular composition, Env. Sci. Techol., 31, 1345–1358, 1997.

Fowlis, I. A.: Gas Chromatography, in: "Analytical Chemistry by Open Learning", John Wiley and Sons, 1995.

Gao, S., Keywood, M., Ng, N. L., Surratt, J., Varutbangkul, V., Bahreini, R., Flagan, R. C., and Seinfeld, J. H.: Low-molecular-weight and oligomeric components in secondary organic aerosol from the ozonolysis of cycloalkenes and alpha-pinene, J. Phys. Chem. A., 108, 10 147–10 164, 2004a.

Gao, S., Ng, N. L., Keywood, M., Varutbangkul, V., Bahreini, R., Nenes, A., He, J. W., Yoo, K. Y., Beauchamp, J. L., Hodyss, R. P., Flagan, R. C., and Seinfeld, J. H.: Particle phase acidity and oligomer formation in secondary organic aerosol, Env. Sci. Techol., 38, 6582–6589, 2004b.

Hamilton, J. F., Webb, P. J., Lewis, A. C., Hopkins, J. R., Smith, S., and Davy, P.: Partially oxidised organic components in urban aerosol using GCXGC-TOF/MS, Atmos. Chem. Phys., 4, 1279–1290, 2004.

Hamilton, J. F., Webb, P. J., Lewis, A. C., and Reviejo, M. M.: Quantifying small molecules in secondary organic aerosol formed during the photo-oxidation of toluene with hydroxyl radicals, Atmos. Env., 39, 7263–7275, 2005.

Hastings, W. P., Koehler, C. A., Bailey, E. L., and De Haan, D. O.: Secondary organic aerosol formation by glyoxal hydration and oligomer formation: Humidity effects and equilibrium shifts during analysis, Env. Sci. Techol., 39, 8728–8735, 2005.

Jang, M. S. and Kamens, R. M.: Characterization of secondary aerosol from the photooxidation of toluene in the presence of NOx and 1-propene, Env. Sci. Techol., 35, 3626–3639, 2001.

Kalberer, M., Paulsen, D., Sax, M., Steinbacher, M., Dommen, J., Prevot, A. S. H., Fisseha, R., Weingartner, E., Frankevich, V., Zenobi, R., and Baltensperger, U.: Identification of polymers as major components of atmospheric organic aerosols, Science, 303, 1659–1662, 2004.

Kalberer, M., Sax, M., and Samburova, V.: Characterization of polymers in nanometer sized atmospheric aerosol particles, Chimia, 59, 43–43, 2005.

Kalberer, M., Yu, J., Cocker, D. R., Flagan, R. C., and Seinfeld, J. H.: Aerosol formation in the cyclohexene-ozone system, Env. Sci. Techol., 34, 4894–4901, 2000.

Kimura, M., Hasegawa, Y., Nakagawa, K., Kajita, M., Watanabe, K., and Yamaguchi, S.: A sensitive method for 4-hydroxybutyric acid in urine using gas chromatography-mass spec-

trometry, J. Chromatogr., B: Anal. Technol. Biomed. Life Sci., 792, 141–144, 2003.

Putaud, J. P., Raes, F., Van Dingenen, R., Bruggemann, E., Facchini, M. C., Decesari, S., Fuzzi, S., Gehrig, R., Huglin, C., Laj, P., Lorbeer, G., Maenhaut, W., Mihalopoulos, N., Mulller, K., Querol, X., Rodriguez, S., Schneider, J., Spindler, G., ten Brink, H., Torseth, K., and Wiedensohler, A.: European aerosol phenomenology-2: chemical characteristics of particulate matter at kerbside, urban, rural and background sites in Europe, Atmos. Env., 38, 2579–2595, 2004.

Saxena, P. and Hildemann, L. M.: Water-soluble organics in atmospheric particles: A critical review of the literature and application of thermodynamics to identify candidate compounds, J. Atmos. Chem., 24, 57–109, 1996.

Talbot, R. W., Andreae, M. O., Andreae, T. W., and Harriss, R. C.: Regional Aerosol Chemistry of the Amazon Basin During the Dry Season, J. Geophys. Res., 93, 1499–1508, 1988.

Tolocka, M. P., Jang, M., Ginter, J. M., Cox, F. J., Kamens, R. M., and Johnston, M. V.: Formation of oligomers in secondary organic aerosol, Env. Sci. Techol., 38, 1428–1434, 2004.

Table 1. Low molecular weight reaction products identified in cyclohexene ozonolysis SOA using GCXGC-TOF/MS.

Identified analyte	Mass	Peak on GCXGC	Structure
LINEAR			
ALDEHYDES and KETONES			
butanal	72	1	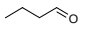
pentanal	86	3	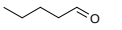
hexanal	100	4	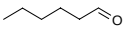
2-propenal	56		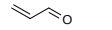
2-butenal	70		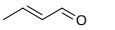
2-hexenal	98		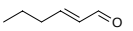
3-hydroxy-butenal	86		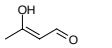
butanedial	86		
hexanedial	114	12	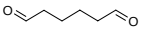
2-hexanone	100		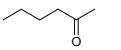
ACIDS			
propanoic acid	74		
butanoic acid	88	6	
pentanoic acid	102	8	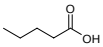
hexanoic acid	116		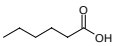
butandioc acid (succinic acid)	118		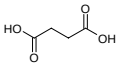
pentandioc acid (glutaric acid)	132	17	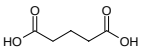
hexandioc acid (adipic acid)	146	18	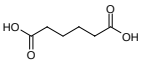

Table 1. Continued.

OTHERS			
butanol	74	2	
2-butene-1,4-diol	88		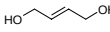
2-butoxyethanol	118		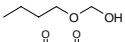
hexanoic acid anhydride	214	20	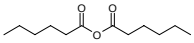
CYCLICS			
Cyclohexanone	98	9	
1,2-cyclohexandione	112		
2-hydroxy-cyclohexanone	114	11	
cyclohexanol	100	7	
1,2-cyclohexandiol	116	15	
formic acid cyclohexyl ester	128		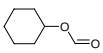
cyclohexen-2-one	96		
1-4-cyclohexen-2-dione	110		
cyclopentanone	84	5	
cyclopentane carboxaldehyde	98		
2-methyl-cyclopentanone	98		
cyclopentenone	82		
cyclopentendione	96		

Table 1. Continued.

dihydro-2(3H)-furanone	86	10	
2(5H)-furanone	84		
dihydro-5-methyl-2(3H)-furanone	100		
2,5-furandione	98		
2,5-dihydro-furandione (succinic anhydride)	100	13	
5-oxotetrahydro-furan-2-carboxylic acid	128	19	
tetrahydro-2H-pyran-2-one	100	14	
dihydro-2H-pyran-2,6-(3H)-dione	114	16	
2-oxepanone	114		
6-oxo-bicyclo[3.1.0]hexan-3-one	98		
7-oxobicyclo[4.1.0]heptane	98		
6,8-dioxabicyclo[3.2.1]octane	114		

Table 2. Low molecular weight reaction products in cyclohexene ozonolysis SOA extract identified using LC-MS/MS.

Identified analyte	[M-H] *m/z* ratio	Mass	Structure
6-Oxo-hexanoic acid	129	130	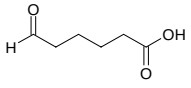
Dioxo-hexanoic acid	145	146	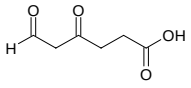
Pentanedioc acid (Glutaric)	131	132	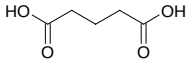
Hexanedioc acid (Adipic)	145	146	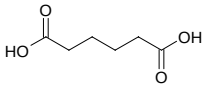
Hydroxy-glutaric acid	147	148	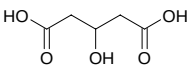
Hydroxy-adipic acid	161	162	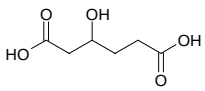
3,6-dihydroxy-5-oxohexanoic acid	161	162	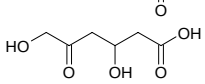

Table 3. Proposed dimer structures of peaks identified in LC-MS/MS chromatogram. Possible molecular formulas and corresponding dimer-monomer pairs are shown for each mass.

Most abundant ion	Molecular weight	Molecular formulas	Example structure	Monomers
231	232	$C_{10}H_{16}O_6$	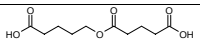	Glutaric acid 5-hydroxy-pentanoic acid
245	246	$C_{11}H_{18}O_6$	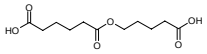	Adipic acid 5-hydroxy-pentanoic acid
		$C_{10}H_{14}O_7$	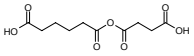	Adipic acid Succinic acid
		$C_9H_{10}O_8$	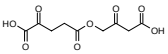	Oxo-glutaric acid 5-hydroxy-oxobutyric acid
		$C_8H_6O_9$	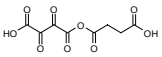	Dioxo-succinic acid Succinic acid
		$C_7H_2O_{10}$	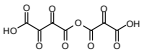	Dioxo-succinic acid Oxo-malonic acid
261	262	$C_{11}H_{18}O_7$	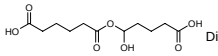	Adpic acid Di-hydroxy-pentanoic acid
		$C_{10}H_{14}O_8$	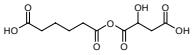	Adipic acid Hydroxy-succinic acid
		$C_9H_{10}O_9$	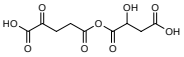	Oxo-glutaric acid Hydroxy-succinic acid
		$C_8H_6O_{10}$	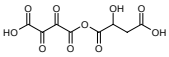	Dioxo-succinic acid Hydroxy-succinic acid
275	276	$C_{12}H_{20}O_7$	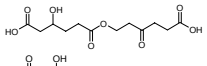	Hydroxy-adipic acid 6-hydroxy-oxohexanoic acid
		$C_{11}H_{16}O_8$	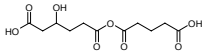	Hydroxy-adipic acid Glutaric acid
		$C_{10}H_{12}O_9$	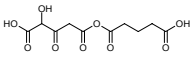	Oxo-hydroxy-glutaric acid Glutaric acid
		$C_9H_8O_{10}$	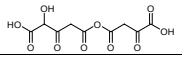	Oxo-hydroxy-glutaric acid Oxo-succinic acid

6389

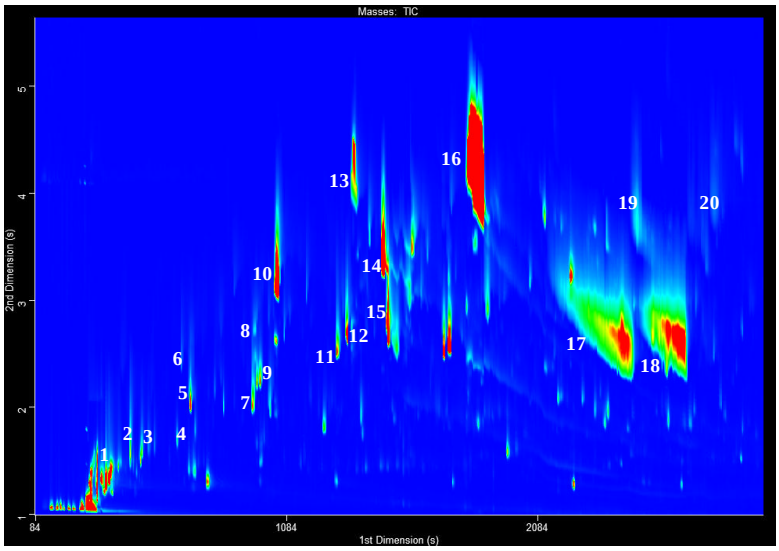

Fig. 1. TIC chromatogram obtained by TD-GCXGC-TOF/MS of a cyclohexene ozonolysis aerosol sample. Peak identifications are given in Table 1.

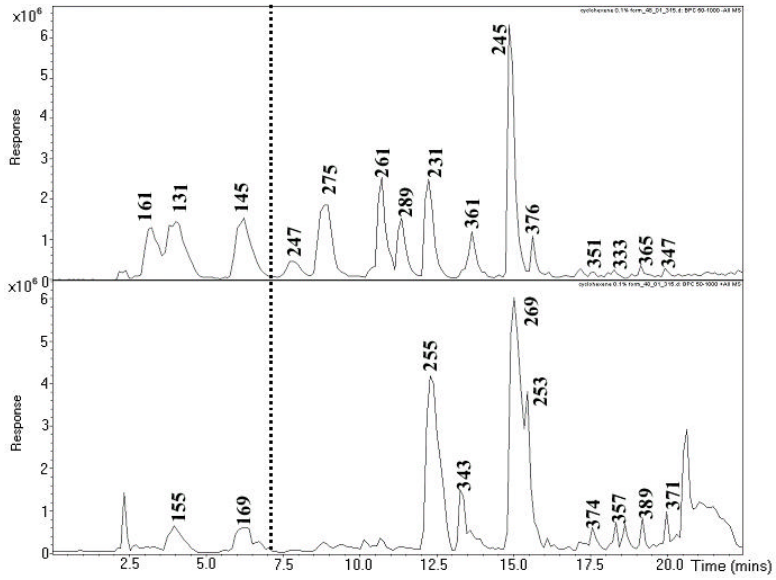

Fig. 2. Electrospray LC-ion-trap MS chromatograms of the cyclohexene SOA methanol extract. Upper: Negative ionisation mode. Lower: Positive ionisation mode. Labels correspond to the most abundant ion for each peak.

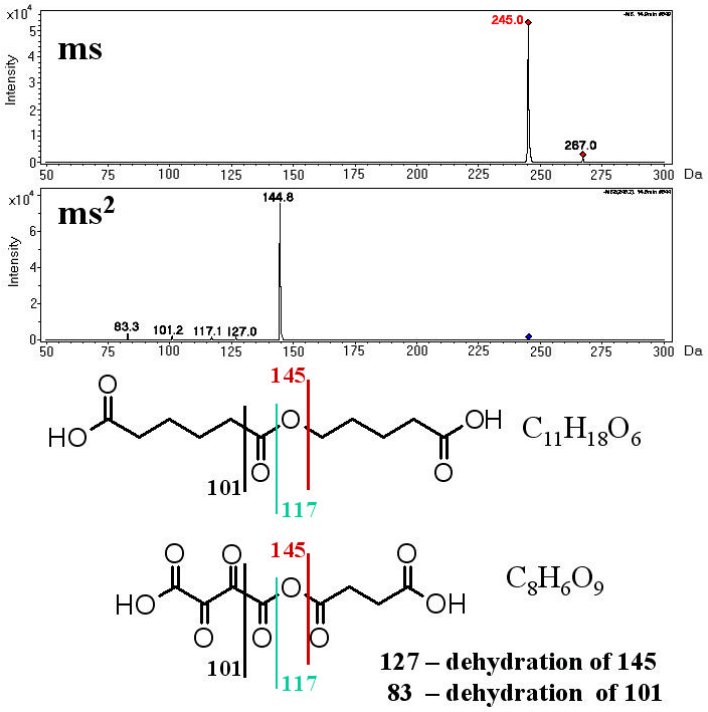

Fig. 3. Mass spectral data and structural analysis of peak with $[M\text{-}H]^-$ of 245 Da. Top: MS spectrum at peak apex. Middle: Collision induced dissociation product ion spectrum. Bottom: Two possible structures that explain the MS^2 fragmentation. High mass resolution spectrometry indicates that the upper structure has the correct molecular formula and is most likely.

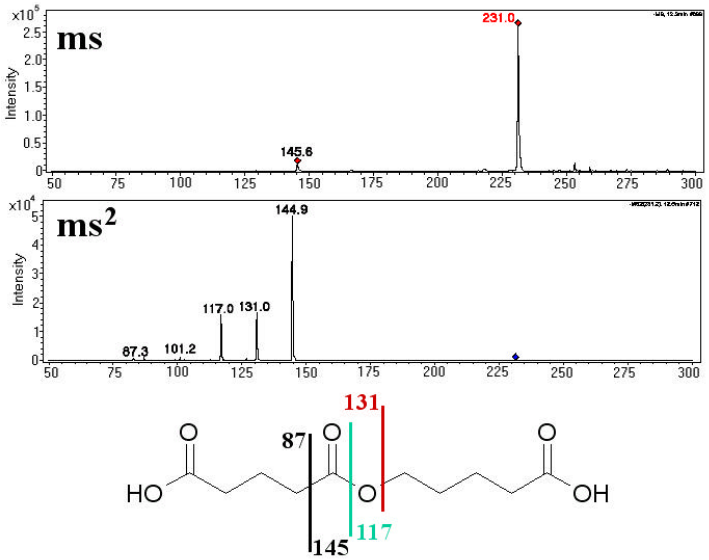

Fig. 4. Mass spectral data and structural analysis of peak with $[M\text{-}H]^-$ of 231 Da. Top: MS spectrum at chromatographic peak apex. Middle: Collision induced dissociation product ion spectrum. Bottom: Proposed structure, fragments that explain MS^2 spectrum are shown.

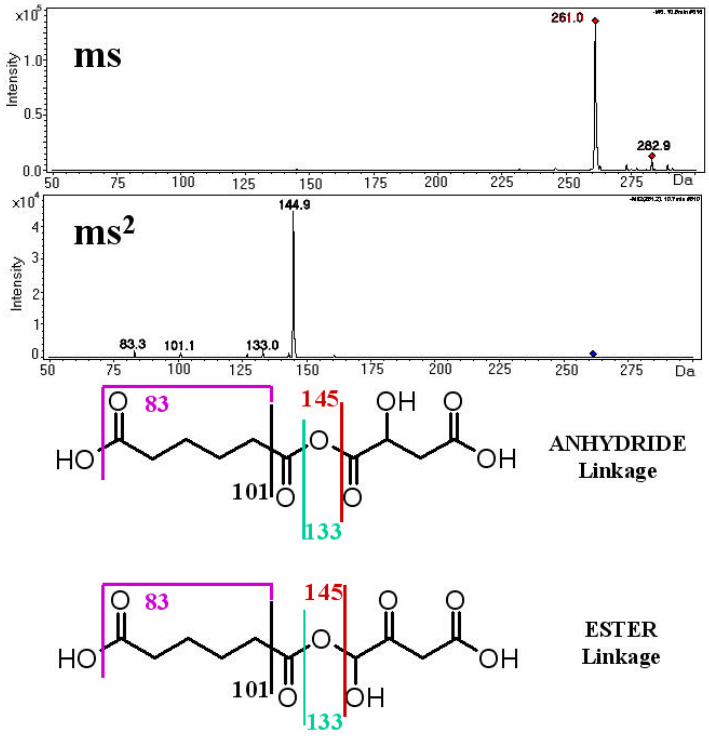

Fig. 5. Mass spectral data and structural analysis of peak with $[M\text{-}H]^-$ of 261 Da. Top: MS spectrum at peak apex. Middle: Collision induced dissociation product ion spectrum. Bottom: Proposed structures with ester (upper) and acid anhydride (lower) linkages. Both structures can explain MS^2 spectrum and have correct molecular formula.

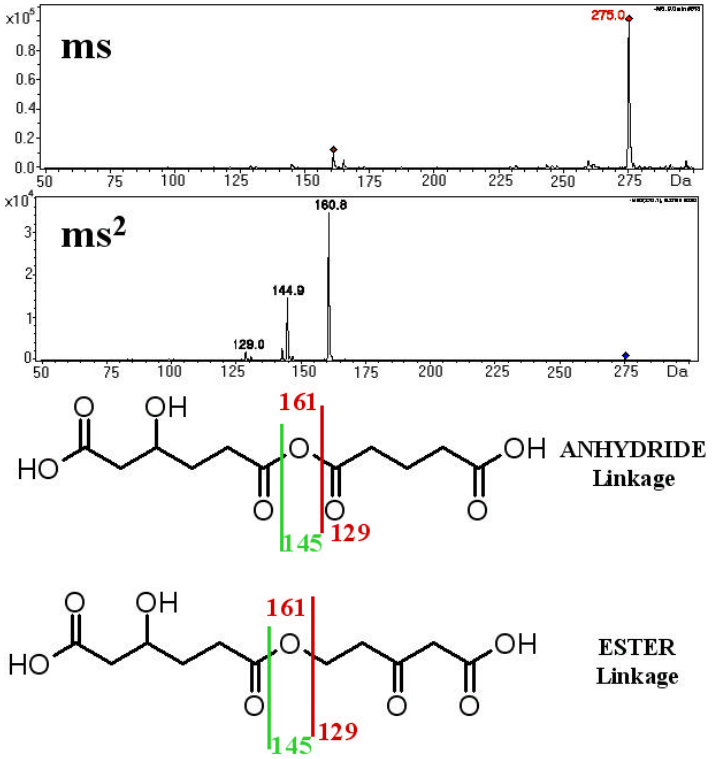

Fig. 6. Mass spectral data and structural analysis of peak with $[M\text{-}H]^-$ of 275 Da. Top: MS spectrum at peak apex. Middle: Collision induced dissociation product ion. Bottom: Proposed structures with ester (upper) and acid anhydride (lower) linkages. Both structures can explain MS^2 spectrum and have correct molecular formula.

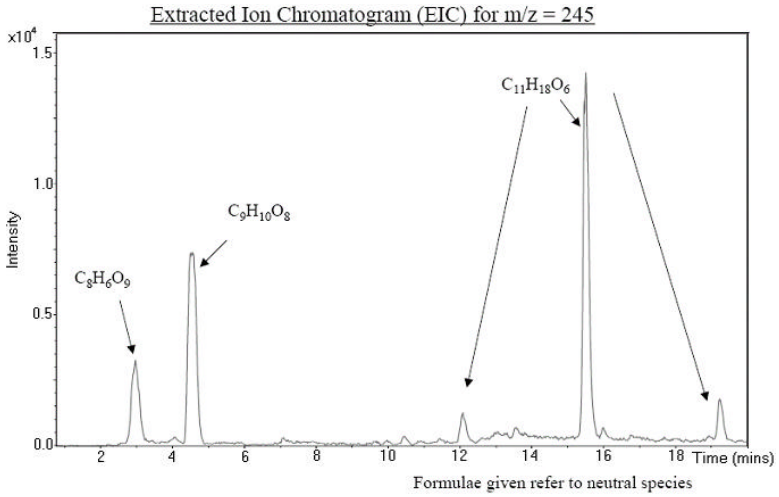

Fig. 7. Extracted ion chromatogram for *m/z* 245, obtained using high resolution micrOTOF detector. Peaks are labelled with the associated molecular formula.

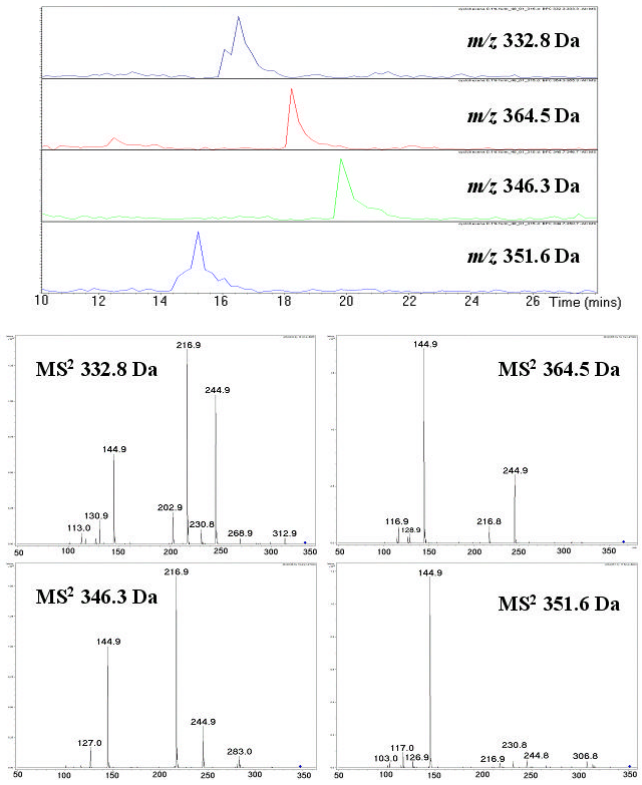

Fig. 8. Upper: Extracted ion chromatograms for m/z 332.8 (black), 264.5 (red), 346.3 (green), and 351.6 Da (blue). Lower: Product ion mass spectrum for each peak.

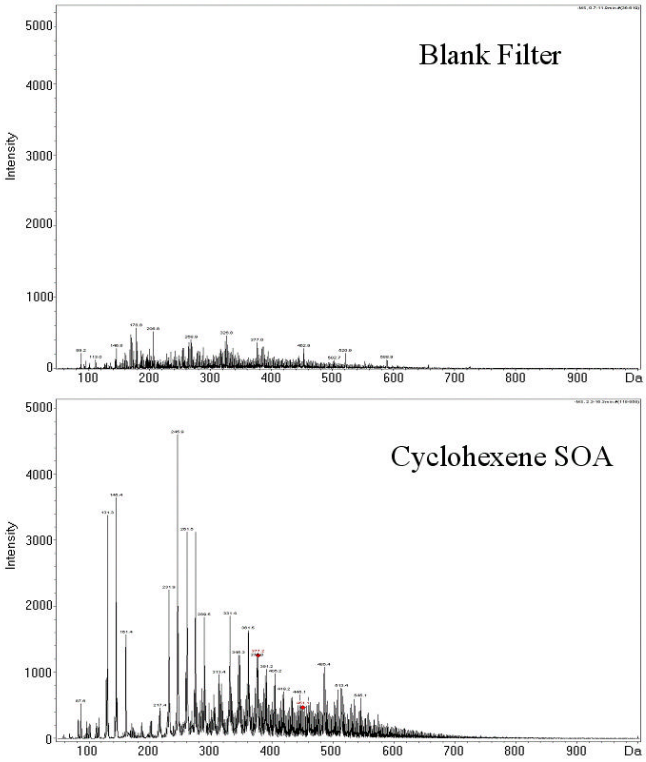

Fig. 9. Averaged mass spectrum across the entire LC chromatogram. Upper: Blank filter. Lower: Cyclohexene ozonolysis aerosol.

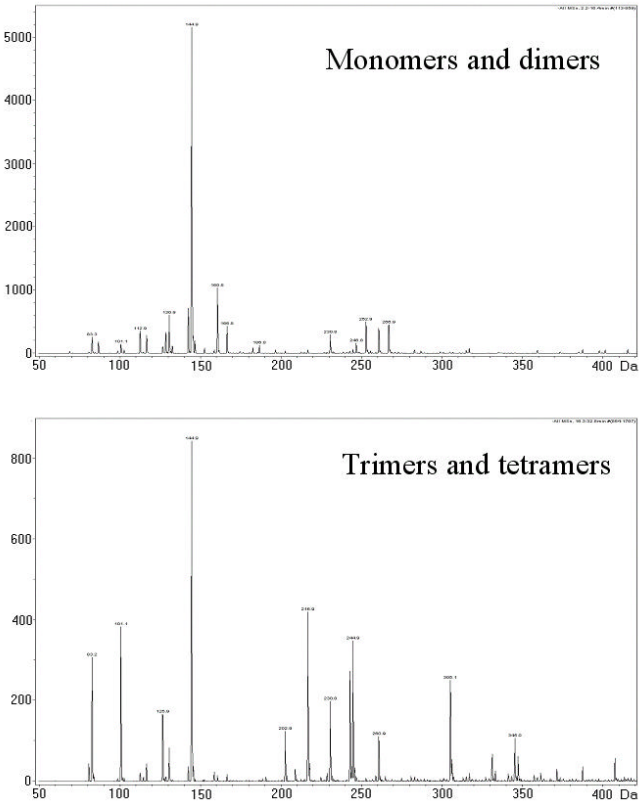

Fig. 10. Average product ion mass spectrum across the entire LC chromatogram. Upper: Monomer and dimer region. Lower: Trimer and tetramers region.